Elementary Morphing Shells: Their Complete Behaviour

Evripides G. LOUKAIDES[1], Corrado MAURINI[2,3] and Keith A. SEFFEN[4]

[1] Department of Engineering, University of Cambridge, Trumpington Street, Cambridge, United Kingdom CB2 1PZ
[2] UPMC Univ Paris 6, UMR 7190, Institut Jean Le Rond d'Alembert, Boite courrier 161, 4 Place Jussieu, F-75005, Paris, France,
[3] CNRS, UMR 7190, Institut Jean Le Rond d'Alembert, Boite courrier 161, 4 Place Jussieu, F-75005, Paris, France
[4] Department of Engineering, University of Cambridge, Trumpington Street, Cambridge, United Kingdom CB2 1PZ, *kas14@cam.ac.uk*

Summary

In this paper, we present a complete overview of possible stable geometries for multistable shells under the uniform curvature assumption. Based on previous work, and using some aspects of Catastrophe Theory we formally identify the boundaries between monostable, bistable and tristable regions and isolate the relevant material and geometrical parameters. The boundaries themselves represent regions of neutral stability, which in turn allow for an infinity of shapes, and we believe these exhaust the possibilities for multistable shells, putting a practical ceiling at a maximum of three states with absolute stability.

Keywords: *morphing; shells; multistable; catastrophe; actuation.*

1. Introduction

In the past few years, much interest has centered on developing multistable shells. Their uses range from children toys to the aeronautical industry and, in Nature, we encounter shell bistability in the snapping of the Venus Flytrap [1]. Recent papers have made substantial contributions towards understanding them and have presented bistable, tristable and neutrally stable behaviour using corrugated, composite and pre-stressed shells ([2],[3],[4]).

Seffen & Guest [5] focussed on specific cases of shells using the same energy formulation presented here, in order to ascribe the effect of initial geometry, constitutive material behaviour and pre-stressing on stability. They obtained closed-form solutions of the deformed, load-free shapes of shell as well as their stability properties—but only for a limited number of cases; here, we aim to extend their results by developing a less restricting strategy to account for all possible initial configurations. Central to this approach is the strain energy potential, which is algebraic in nature owing to the widespread assumption of uniform curvatures. Accordingly, we can operate upon this polynomial expression by employing tools from Catastrophe Theory, to describe conclusively regions of stability—their extent and their boundaries—in terms of controlling parameters of initial shape, material properties and pre-stress. Importantly, we do not have to solve explicitly for all possible equilibria, rather only for them that lie at the interface between differently stable regimes.

This paper aims to show the complete range of behaviour for free-standing multistable shells under the uniform curvature assumption. We also show that the controlling parameters for stability, can be reduced to a few geometric and material parameters. With this simplified expression for the shell energy, we are able to use some tools from Catastrophe Theory to conclusively describe areas a mono-, bi- and tri-stability, and the boundaries between them.

In general, Catastrophe Theory allows us to examine how systems respond to small changes in their controlling parameters. To state this more clearly; if we consider a potential $V(x_i; c_a)$, with n state variables x_i and l control parameters c_a ($1 \leq i \leq n$, $1 \leq a \leq l$), the equilibria, $x_i(c_a)$, can be found by solving:

$$\frac{\partial V(x_i;c_a)}{\partial x_i} = 0 \qquad (i = 1,2,\dots,n) \tag{1}$$

Catastrophe Theory then reveals how the equilibria, or "critical points", $x_i(c_a)$ of $V(x_i; c_a)$ perform as the control parameters, c_a, change [6]. Their stability is assessed using the Hessian matrix of V and, according to Thom's splitting lemma, the interesting behaviour occurs when the Hessian becomes singular. This scenario is called a catastrophe, and original work by Thom [7] classifies all the possible forms for energy potentials described by less than six parameters. As the name implies, these events can sometimes lead to sudden failures in practice, and Catastrophe Theory can help us detect and prevent the generating circumstances. In many other cases, we study the catastrophe event, in order to understand and control a useful transition between stability regimes—as in the multistable shells here, and this might be realised, for example, by embedding actuators in the structure [8].

The outline of this paper is as follows. Section 2 introduces the strain energy potential for multistable shells, which has been developed elsewhere, which is then simplified in Section 3 mainly by eliminating redundant parameters. Section 4 uses some tools from Catastrophe Theory to characterise and distinguish regions of consistent mutltistable behaviour in terms of geometric, material and pre-stress parameters: we also choose to study the stability of one special critical point of interest. In Section 5 we conclude with a summary.

2. Strain energy expression

Our analysis uses the governing equations of deformation for multistable orthotropic shells derived by Seffen [9]. These are for an unloaded, linear elastic shell of elliptical planform and constant thickness. They account for both bending and stretching of the shell middle surface, and their derivation relies upon the assumption of uniform curvatures throughout; there is no spatial variation, which enables the classical governing partial differential equations to be simplified without a loss of accuracy. Although this approach ignores the effect of a narrow and real layer of non-uniform bending at the edge of the shell, the middle-surface forces are exactly determined for this mode of deformation. The final dimensionless expression for the strain energy stored in the shell can be written as a fourth-order polynomial:

$$\bar{U} = \frac{\phi}{2}[\bar{\kappa}_x\bar{\kappa}_y - \bar{\kappa}_{xy}^2 - \bar{\kappa}_{x0}\bar{\kappa}_{y0} + \bar{\kappa}_{xy0}^2]^2 + \frac{1}{2}[(\bar{\kappa}_x - \bar{\kappa}_{x0})^2 + 2\nu(\bar{\kappa}_x - \bar{\kappa}_{x0})(\bar{\kappa}_y - \bar{\kappa}_{y0}) + \beta(\bar{\kappa}_y - \bar{\kappa}_{y0})^2 + 4(1 - \nu^2/\beta)\rho(\bar{\kappa}_{xy} - \bar{\kappa}_{xy0})^2] \tag{2}$$

Here β and ρ are the modular ratios equal to E_y/E_x and G/E_x with Young's modulus, E, and shear modulus, G, and x and y are in-plane coordinates aligned to the major and minor axes of the shell. The Poisson ratio is ν, and ϕ is a geometrical and material shape factor for the shell. The κ terms are the out-of-plane curvatures of the middle surface—our state variables—and they define the current shape of the shell. An overbar denotes a dimensionless form and the other κ terms with a "0" subscript describe the initial stress-free shape.

Pre-stress effects are simply included by replacing the initial curvature with a term equal to the the sum of initial curvature and pre-stress curvature [10]. The latter is the curvature that would be adopted by the shell if it could deform without constraint, and we denote this effect with subscript "F". We also substitute the shear stiffness term with a single parameter for convenience, and our slightly modified potential compared to Seffen & Guest [5] can be read as:

$$\bar{U} = \frac{\phi}{2}[\bar{\kappa}_x\bar{\kappa}_y - \bar{\kappa}_{xy}^2 - \bar{\kappa}_{x0}\bar{\kappa}_{y0} + \bar{\kappa}_{xy0}^2]^2 + \frac{1}{2}[(\bar{\kappa}_x - \bar{\kappa}_{x0} - \bar{\kappa}_{xF})^2 + 2\nu(\bar{\kappa}_x - \bar{\kappa}_{x0} - \bar{\kappa}_{xF})(\bar{\kappa}_y - \bar{\kappa}_{y0} - \bar{\kappa}_{yF}) + \beta(\bar{\kappa}_y - \bar{\kappa}_{y0} - \bar{\kappa}_{yF})^2 + 4\alpha(\bar{\kappa}_{xy} - \bar{\kappa}_{xy0} - \bar{\kappa}_{xyF})^2] \tag{3}$$

3. Removal of redundant parameters

Catastrophe Theory allows us to examine the strain energy potential in view of its global stability characteristics. Beforehand, we simplify Eqn 3 by isolating those parameters directly responsible for controlling multistability: any other parameters that do not are given a nominal value, as now described.

First, we transform the dimensionless curvatures by setting $\bar{\kappa}_x = \hat{\kappa}_x\sqrt{\beta}$, with similar transformations for the "F" and "0" subscripts: none is needed for the y-direction terms. For the terms associated with twisting, we substitute $\bar{\kappa}_{xy} = \hat{\kappa}_{xy}\sqrt[4]{\beta}$, and β can be eliminated by introducing

new variables, namely: $\gamma = 4\alpha\sqrt{\beta},\ \ \lambda = \nu\sqrt{\beta},\ \bar{\phi} = \phi\sqrt{\beta}$. This shows that β is simply a scaling factor for the strain energy, which can be set to unity without changing the stability properties of the shell. Similarly for $\bar{\phi}$, we apply an isotropic transformation such that $\hat{\kappa} = \tilde{\kappa}/\sqrt{\bar{\phi}}$, and we re-cast the strain energy by defining $\widetilde{U} = \bar{\phi}\overline{U}$. As a result, $\bar{\phi}$ emerges as another linear scaling factor, which is also set equal to unity, for convenience.

In addition, we combine the initial curvatures and pre-stress into three control parameters by setting $h_x = \hat{\kappa}_{x0} + \hat{\kappa}_{xF}$, $h_y = \hat{\kappa}_{y0} + \hat{\kappa}_{yF}$ and $g_0 = \hat{\kappa}_{x0}\hat{\kappa}_{y0}$, the initial Gaussian curvature. Control parameters related to twist are set equal to zero following a separate study, which has confirmed that their effect upon the overall stability landscape is marginal. However, the twisting curvature must be retained as a state variable for propriety in assessing stability. Substituting the new variables, we obtain the required form of strain energy potential as:

$$\widetilde{U} = \tfrac{1}{2}[\tilde{\kappa}_x\tilde{\kappa}_y - \tilde{\kappa}_{xy}^2 - g_0]^2 + \tfrac{1}{2}[(\tilde{\kappa}_x - h_x)^2 + 2\lambda(\tilde{\kappa}_x - h_x)(\tilde{\kappa}_y - h_y) + (\tilde{\kappa}_y - h_y)^2 + \gamma\tilde{\kappa}_{xy}^2] \quad (4)$$

We now have an equivalent system whose control parameters are g_0, h_x, h_y, γ and λ.

3.1 Stability

The stability of each state can be examined through the generalised stiffness matrix. This is produced from the Taylor expansion of the generalised energy expression, where a form is given by Guest & Pellegrino [11], and then extended by Seffen [9]. There are three state variables, and the complete matrix is written as:

$$H = \mathrm{Hess}(\widetilde{U}) = \begin{bmatrix} \dfrac{\partial^2\widetilde{U}}{\partial\tilde{\kappa}_x^2} & \dfrac{\partial^2\widetilde{U}}{\partial\tilde{\kappa}_x\,\partial\tilde{\kappa}_y} & \dfrac{\partial^2\widetilde{U}}{\partial\tilde{\kappa}_x\,\partial\tilde{\kappa}_{xy}} \\ \dfrac{\partial^2\widetilde{U}}{\partial\tilde{\kappa}_y\,\partial\tilde{\kappa}_x} & \dfrac{\partial^2\widetilde{U}}{\partial\tilde{\kappa}_y^2} & \dfrac{\partial^2\widetilde{U}}{\partial\tilde{\kappa}_y\,\partial\tilde{\kappa}_{xy}} \\ \dfrac{\partial^2\widetilde{U}}{\partial\tilde{\kappa}_{xy}\,\partial\tilde{\kappa}_x} & \dfrac{\partial^2\widetilde{U}}{\partial\tilde{\kappa}_{xy}\,\partial\tilde{\kappa}_y} & \dfrac{\partial^2\widetilde{U}}{\partial\tilde{\kappa}_{xy}^2} \end{bmatrix}$$

$$= \begin{bmatrix} 1+\tilde{\kappa}_y^2 & \lambda - g_0 + 2\tilde{\kappa}_x\tilde{\kappa}_y - \tilde{\kappa}_{xy}^2 & -2\,\tilde{\kappa}_{xy}\tilde{\kappa}_y \\ \lambda - g_0 + 2\tilde{\kappa}_x\tilde{\kappa}_y - \tilde{\kappa}_{xy}^2 & 1+\tilde{\kappa}_x^2 & -2\,\tilde{\kappa}_{xy}\tilde{\kappa}_x \\ -2\,\tilde{\kappa}_{xy}\tilde{\kappa}_y & -2\,\tilde{\kappa}_{xy}\tilde{\kappa}_x & 6\tilde{\kappa}_{xy}^2 - 2\tilde{\kappa}_x\tilde{\kappa}_y + 2g_0 + \gamma \end{bmatrix} \quad (5)$$

after substituting Eqn (3), and differentiating appropriately. An equilibrium solution is stable when H is positive definite, and a sufficient condition is that all the eigenvalues of H are positive. When there is a change in the stability performance, it is marked by some of the eigenvalues reducing to zero.

4. Analysis of different parameter regions

4.1 Overview of stability regions

In order to establish the stability performance, previous studies— typically carried out by engineers—find the equilibrium shapes of shell explicitly and then check their stability using H. To extract any dependence of the stability upon the initial parameters, an exhaustive approach is performed involving all possible values and combinations of them, and the results are then presented in some suitable graphical form that reveals the transition between regimes. In Catastrophe Theory, these transitions are termed the "critical boundaries", and they are obtained more efficiently for two reasons: by focusing on the influence of the controlling parameters, rather than the state variables, and by only dealing with equilibria on these boundaries. In the present case, these boundaries are found by formally solving the following system of four equations:

$$\frac{\partial\widetilde{U}}{\partial\tilde{\kappa}_x} = 0 \qquad \frac{\partial\widetilde{U}}{\partial\tilde{\kappa}_y} = 0 \qquad \frac{\partial\widetilde{U}}{\partial\tilde{\kappa}_{xy}} = 0 \quad (6)$$

$$|H| = 0. \quad (7)$$

Eqns 6 detect equilibria as points of minimum energy with respect to the shell geometry, material properties and pre-stress. These can be solved in closed-form in terms of the state variables and the control parameters, and the resulting expressions are substituted into Eqn 7, which determines the critical boundaries directly. Some simplification is obtained if we express the curvatures in a new coordinate system (κ_m, κ_d), such that $\tilde{\kappa}_x = \kappa_m + \kappa_d$, $\tilde{\kappa}_y = \kappa_m - \kappa_d$. Similarly, $h_x = h_m + h_d$, $h_y = h_m - h_d$. The closed form solutions of Eqns 6 can be verified as:

$$-2(\kappa_m(-1 + g_0 + \kappa_d^2 - \kappa_m^2 + \kappa_{md}^2 - \lambda) + h_m(1 + \lambda)) = 0 \quad (8a)$$

$$2(\kappa_d(1 + g_0 + \kappa_d^2 - \kappa_m^2 + \kappa_{md}^2 - \lambda) + h_d(-1 + \lambda)) = 0 \quad (8b)$$

$$\kappa_{md}(\gamma + 2g_0 + 2\kappa_d^2 - 2\kappa_m^2 + 2\,\kappa_{md}^2) = 0 \quad (8c)$$

We see from Eqn 8(c) that twisted and untwisted solutions are uncoupled. We also observe that γ does not affect the form of untwisted equilibria. It does however affect their stability. In addition, when we do include twisted solutions, γ has an effect. For a more detailed analysis of this, see Fernandes *et al* [12]. We focus on untwisted solutions to allow us a simpler overview of overall behaviour. We set $\kappa_{md} = 0$, and the remaining three equations – 7, 8(a), 8(b) - contain six unknowns in $\kappa_m, \kappa_d, h_m, h_d, g_0$ and λ. We choose to specify λ, the Poisson's ratio term, and g_0, the initial dimensionless Gaussian curvature, because we are interested specifically in the effects of pre-stress: this reduces the number of unknowns to four, thereby enabling unique, parametric solutions for the remaining parameters. Their final expressions are obtained using the symbolic solver in Mathematica [13]. We give compact expressions for h_d and h_m below with κ_d as the parametric variable. In total, there are four of them, depending on the choice of sign within "$\pm$", and they define the relationships between parameters on the critical boundaries:

$$h_m = \pm\frac{\sqrt{-3\sqrt{12\kappa_d^2+(g_0-\lambda+2)^2}+9\kappa_d^2+6g_0-6\lambda+3}\left(\sqrt{12\kappa_d^2+(g_0-\lambda+2)^2}+g_0-\lambda-4\right)}{9(\lambda+1)} \quad (9a)$$

$$h_d = -\frac{\kappa_d\left(\sqrt{12\kappa_d^2+(g_0-\lambda+2)^2}+g_0-\lambda+2\right)}{3(\lambda-1)} \quad (9b)$$

and

$$h_m = \pm\frac{\sqrt{\sqrt{12\kappa_d^2+(g_0-\lambda+2)^2}+3\kappa_d^2+2g_0-2\lambda+1}\left(\sqrt{12\kappa_d^2+(g_0-\lambda+2)^2}-g_0+\lambda+4\right)}{3\sqrt{3}(\lambda+1)} \quad (10a)$$

$$h_d = \frac{\kappa_d\left(\sqrt{12\kappa_d^2+(g_0-\lambda+2)^2}-g_0+\lambda-2\right)}{3(\lambda-1)} \quad (10b)$$

After substituting for κ_d, we can plot these expressions on the (h_x, h_y) plane for specified values of λ and g_0, which returns the critical boundaries as certain curves. By repeating this process for a range of g_0 values, for the same value of λ, successive (h_x, h_y) planes can be assembled in the direction of g_0, to render the critical boundaries as *surfaces* in Cartesian space of axes (h_m, h_d, g_0). One set of surfaces is given in Fig. 1 and the volumetric space between surfaces corresponds to the values of pre-stress and initial shape needed to yield equilibria of the same stability properties. To find out the degree of stability, we plot some of the original horizontal slices in Fig. 2. They clearly show the boundary curves and the junction, or "critical", points at which they intersect, and how they evolve with g_0. By considering the topological features of the boundary curves in the vicinity of the critical points, we can pronounce directly upon the degree of stability around them using Thom's classification [8]. In particular, the pitchfork bifurcation, which manifests as a cusp catastrophe, marks the transition from monostable to bistable regions along the $h_m = 0$ and $h_d = 0$ lines. In Fig. 2 we see, for different values of the initial Gaussian curvature, the outline of all curves indicating loss of equilibria or stability on the h_m-h_d plane.

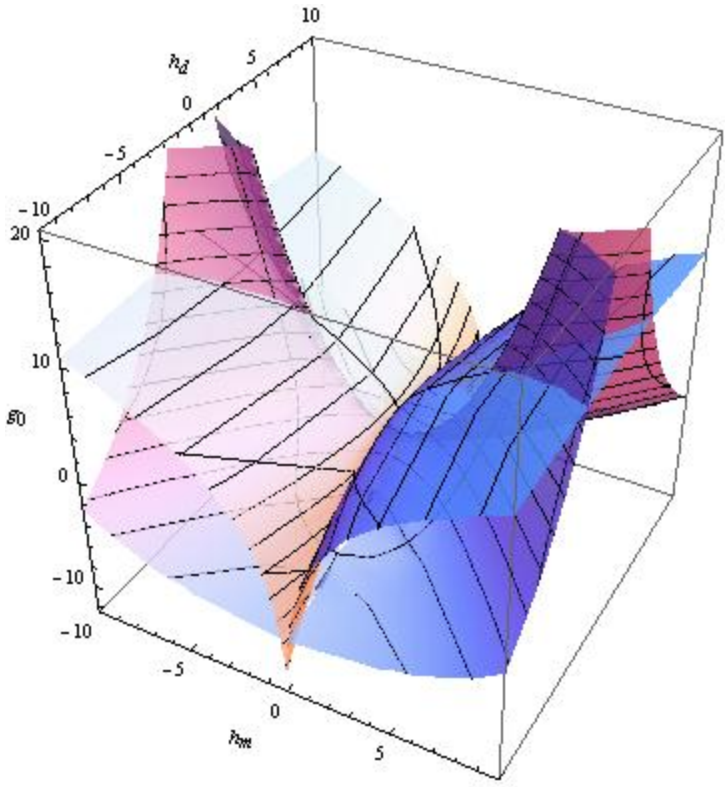

Figure 1: All possible stability states are summarized in this diagram. The surfaces shown are the critical boundaries from the system of Eqns 6 and 7. They define transitional surfaces. We allow a range of values for the parametric variable, such that $-10 < \kappa_d < 10$*. We also fix* λ *at 0,3. Each surface divides the parameter space in multistable and monostable regions. With reference to the point of view in this diagram, the volume above the top set of surfaces and below the bottom set of surfaces is bistable. The volume where the two bistable regions overlap, describes the tristable region. This feature is prominent here at the four sides of the diagram. The remaining space between the surfaces shows monostable regions. Since we are dealing with shallow shells, we choose to display a region close to the origin. Expanding this range however does not reveal further detail.*

There are only four critical points that allow passage from monostable to tristable regions and their location is of interest. Based on previous knowledge [1] and on the symmetry in the energy expression above, we know that moving along $h_y = \pm h_x$, or equivalently, by setting $h_d = 0$ and $h_m = 0$, we can locate those points. We solve Eqns 6 and 7 again but including these constraints, and the resulting solutions for κ_d are found to be:

$$\kappa_d = \frac{\sqrt{\lambda - 1 - g_0}}{\sqrt{3}}, \qquad \kappa_d = -\sqrt{\lambda + 1 - g_0} \tag{11}$$

on the negative h_d axis,

$$\kappa_d = -\frac{\sqrt{\lambda - 1 - g_0}}{\sqrt{3}}, \qquad \kappa_d = +\sqrt{\lambda + 1 - g_0} \tag{12}$$

on the positive h_d axis, and

$$\kappa_d = 0 \tag{13}$$

on $h_d = 0$. These describe the shapes of equilibria when $h_x = \pm h_y$, and the expediting conditions for g_0 and λ can be obtained from substituting the above back into Eqns 9 and 10 to reveal:

$$g_0 = \lambda + 7 \qquad g_0 = \lambda - 2 \tag{14}$$

on $h_d = 0$. The solution $\lambda - 2$ can be dismissed since it produces imaginary curvatures. On $h_m = 0$, we get

$$g_0 = \lambda - 7 \tag{15}$$

Correspondingly, each of the four cusp critical points are identified in terms of λ as

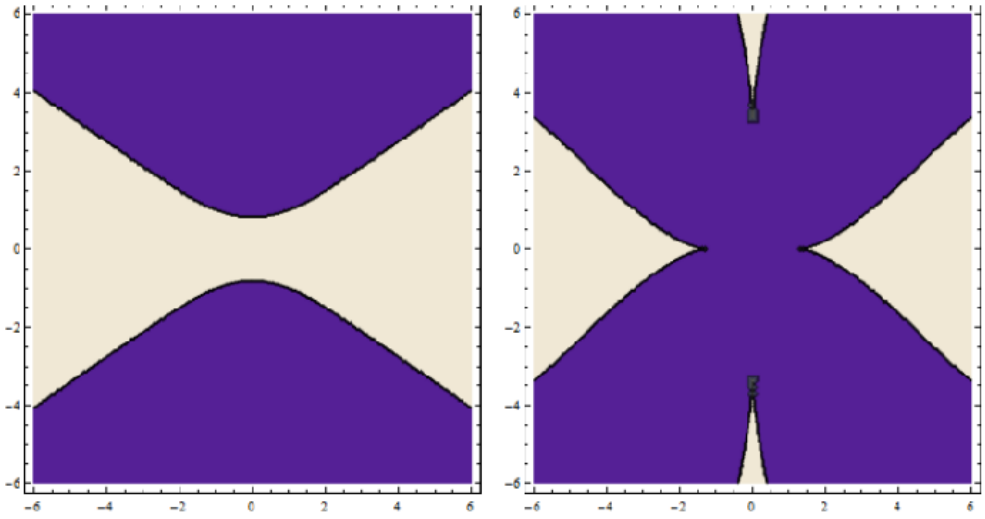

(a) $g_0 < \lambda - 1$ (b) $\lambda - 1 < g_0 < \lambda + 1$

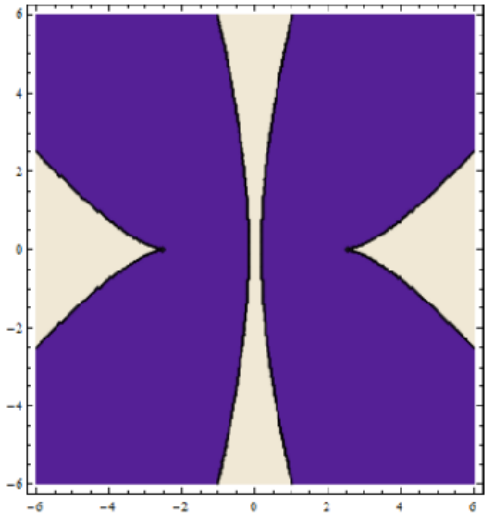

(c) $g_0 > \lambda + 1$

Figure 2: Colormaps showing the number of stable states across the h_m-h_d plane. These were obtained by numerically solving for the curvature and checking the stability via the Hessian matrix of the energy. By varying g_0, we can confirm the critical boundary curves described parametrically in Eqns 12-15. Purple shows monostable regions while white shows bistable regions. The characteristic projection of the cusp catastrophe can be seen in (b) and (c). The parameter λ is constant with value 0,3, and γ is set at 3,64. The initial Gaussian curvature has a tremendous effect on the stability of feasible solutions. For low, negative values of g_0, bistability is mostly observed near $h_d = 0$. As we increase g_0, bistable behavior diminishes along that line and increases along $h_m = 0$.

$$(h_m, h_d, g_0) = \left(\pm\frac{4\sqrt{2}}{0{,}3+1}, 0, (7+0{,}3)\right), \left(0, \pm\frac{4\sqrt{2}}{0{,}3-1}, (7+0{,}3)\right) \quad (16)$$

These points are significant in various ways, but most prominently because they show parameter values where all three possible stability regions meet. They also indicate the extreme values of our parameters that allow tristability.

4.2 Stability near the cusp catastrophe

Returning to the strain energy expression, Eqn 4, we can study the stability of the shell at the vicinity of the cusp catastrophe. We previously explained how Eqn 5 is used to established stability of equilibria. This is straightforward for non-critical points. However at critical points, where the

stability matrix is zero by definition, further calculation is needed. We offer an example by studying the stability of a solution at one of the cusp catastrophe points we have calculated above.

Solving for the curvatures, we get $(\kappa_m^*, \kappa_d^*) = (2\sqrt{2}, 0), (-\sqrt{2}, 0)$, and these identify those values of state variables around which we expand the strain energy expression. This is achieved by specifying sliding coordinates δ_m and δ_d, with $\kappa_m = \kappa_m^* + \delta_m\varepsilon$ and $\kappa_d = \kappa_d^* + \delta_d\varepsilon$. The final form of energy for the first solution is given by:

$$U_s = \text{constant} + \left(2h_d\delta_d(\lambda - 1) + 2\delta_m\left(-\lambda h_m - h_m + 4\sqrt{2}\right)\right)\varepsilon + 18\delta_m^2\varepsilon^2 + 4\sqrt{2}\delta_m(\delta_m^2 - \delta_d^2)\varepsilon^3 + \frac{1}{2}(\delta_d^2 - \delta_m^2)^2\varepsilon^4 + O[\varepsilon^7] \quad (17)$$

The constant and first order terms can be ignored since they do not affect stability. The coefficient of the second order of the expansion is $18\delta_m^2$, which shows that we have stability in the m direction, but the stability in the d direction is undetermined. This is shown graphically in Fig. 3(a). To investigate this further we look at the coefficient of the third order. This is equal to $4\sqrt{2}\delta_m(\delta_m^2 - \delta_d^2)^2$. The third order coefficients are plotted in Fig. 3(b). With respect to the δ_d, the third order coefficient shows this shell geometry to be unstable at the catastrophe point. Similarly, we can draw the same conclusion for the second equilibrium point. Loss of stability at cusp critical points is typical, as explained by Thompson & Hunt (1984) [14].

This result is useful for understanding actuation between shells of different stability properties. In practical terms, if we wanted to have a morphing shell that can act as both a monostable, and a multistable structure, we would need to manipulate our parameters and pass through this exact point in the parameter space. This brief examination shows however, that the structure would not be stable at this point.

5. Conclusions

This work has presented the landscape of possible stable geometries for uniformly curved shells. We have shown conclusively that the maximum number of stable states is three, and we have determined the conditions responsible for the transition between regions of multistability in terms of material parameters, pre-stress and initial shape. Specifically, we note that double initial curvature is always a prerequisite for tristability and that a minimum threshold exists for the Poisson ratio, below which tristability cannot be observed. A more thorough analysis of the influence of each parameter, and most notably of the shear stiffness, is the subject of current research and will be presented elsewhere.

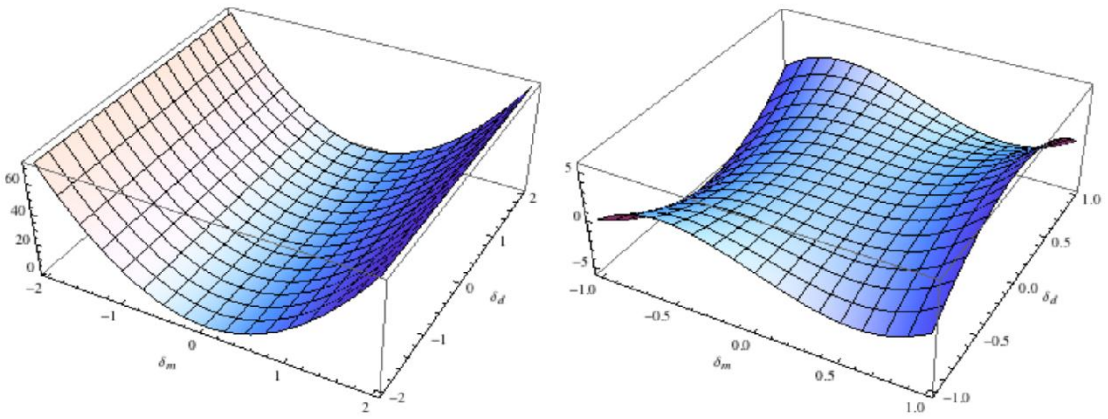

(a) Second order coefficient (b) Third order coefficient

Figure 3: We find the Taylor expansion of the energy expression near the critical point that separates the monostable and tristable regions along $h_d = 0$. The coefficients of the second and third orders of the expansion are in terms of δ_d and δ_m and are plotted here.

6. Acknowledgments

E.G. Loukaides acknowledges financial support from the Alexander S. Onassis Public Benefit Foundation and from the Cyprus State Scholarship Foundation.

7. References

[1] Forterre Y, Skotheim J, Dumais J, and Mahadevan L, "Mechanics of Venus' Flytrap Closure", *In ICTAM04 Proceedings, Warsaw, Poland*, 2004.

[2] Norman A, Seffen K, and Guest S, "Morphing of curved corrugated shells", *International Journal of Solids and Structures*, Vol. 46, 2009, pp. 1624-1633.

[3] Guest SD, Kebadze E, and Pellegrino S, "A Zero-Stiffness Elastic Shell Structure", *Journal of Mechanics of Materials and Structures*, Vol. 6, No. 1-4, 2011, pp. 203-212.

[4] Kebadze E, Guest SD, and Pellegrino S, "Bistable prestressed shell structures", *International Journal of Solids and Structures*, Vol. 41, No. 7-8, 2004, pp. 2801-2820.

[5] Seffen KA, and Guest S, "Prestressed Morphing Bistable and Neutrally Stable Shells", *Journal of Applied Mechanics, ASME*, Vol. 78, No. 1, 2011, pp. 011002-1 to 011002-6.

[6] Gilmore R, *Catastrophe theory for scientists and engineers*. Dover Publications, 1981, p. 5.

[7] Thom R, *Structural stability and morphogenesis*, Addison Wesley Publishing Company, 1975.

[8] Vidoli S, and Maurini C, "Tristability of thin orthotropic shells with uniform initial curvature", *Proceedings of the Royal Society A: Mathematical, Physical and Engineering Science*, Vol. 464, No. 2099, 2008, p. 2949.

[9] Seffen KA, "Morphing bistable orthotropic elliptical shallow shells", *Proceedings of the Royal Society A: Mathematical, Physical and Engineering Science*, Vol. 463, No. 2077, 2007, pp. 67-84.

[10] Seffen KA, "Multistable Anisotropic Shells: Governing Equations of Deformation", *Technical Report CUED/D-STRUCT/TR 225*, Department of Engineering, University of Cambridge, 2008.

[11] Guest S, and Pellegrino S, "Analytical models for bistable cylindrical shells", *Proceedings of the Royal Society A: Mathematical, Physical and Engineering Science*, Vol. 462, No. 2067, 2006, pp. 839-854.

[12] Fernandes A, Maurini C, and Vidoli S, "Multiparameter actuation for shape control of bistable composite plates", *International Journal of Solids and Structures*, Vol. 47, No. 10, 2010, pp. 1449-1458.

[13] Wolfram Research, Inc., *Mathematica*, Wolfram Research, Inc., Champaign, Illinois,Version 7.0, 2008.

[14] Thompson JMT, and Hunt GW, *Elastic Instability Phenomena*, Wiley-Interscience Publication, 1984, pp. 75-76.